Green Synthesis of Cu-Doped Aluminium Hydroxide Sludge Using Lavender for Adsorption of Reactive Azo Dye: A Waste-to-Resource Approach

Aydın, Nesli*[*+•]*; Bacak, Eda; Güneş, Elçin; İzlen Çifçi, Deniz
Department of Environmental Engineering, Faculty of Engineering,
Tekirdağ Namık Kemal University, Çorlu, Tekirdağ, TURKEY

ABSTRACT: *As waste management becomes a competitive sector, it is evident that international guidelines will further encourage the reuse of waste materials. While aluminium hydroxide sludge (AHS) is a problematic waste associated with health and environmental impacts, it is also a valuable material in terms of treating textile wastewater. This paper focuses on the green synthesis of Cu-doped AHS using lavender extract for the adsorption of a reactive azo dye, Remazol Red (RR)239. Results of SEM and FT-IR analyses show that AHS is in the form of aluminium hydroxide and its chemical structure comprises approximately 9.88±0.56% C, 63.39±0.63% O, 21.94±0.10% Al, and 4.04±0.14% S content by weight. Adsorption studies demonstrated that the lowest RR239 uptake was 18.7% at pH 11, while it increased as the pH value decreased to 7. It was also determined that RR239 dye adsorption with Cu-AHS is more suited to pseudo 2nd-order kinetics. The comparison of the RR239 dye uptake capacities of Cu-AHS and AHS adsorbent exhibited that there is a great reduction in RR239 dye removal of Cu-AHS and AHS adsorbents after 75 mg/L RR239 dye concentration. However, across all concentrations, Cu-AHS exhibited a higher RR239 dye uptake capacity than that of AHS. Adsorption isotherms also presented that the dye adsorption of AHS and Cu-AHS is more suitable for the Langmuir isotherm. The environmental advantages of the green synthesis method used in this study and the outstanding capacity of AHS in RR239 dye removal are vital in terms of guiding other studies in waste management.*

KEYWORDS: *Adsorption, Aluminium hydroxide sludge, Green synthesis, Reactive dye, Waste management.*

INTRODUCTION

The rapid increase in commercial waste, such as metal hydroxide sludge being produced largely from aluminium industry, and the scarcity of traditional landfill capacity have become a major concern for industrialised countries. In search of an urgent solution to this situation, authorities introduced new principles under the name of *extended producer responsibility*, which regulates producers' responsibilities for waste disposal costs and sets recycling and reuse targets [1,2]. These expanded responsibilities will be reflected in many areas of production activities and

* *To whom correspondence should be addressed.*
+ E-mail: naydin@nku.edu.tr
1021-9986/2023/11/3707-3719 13/$/6.03
● *Another Address: Karabuk University, Faculty of Engineering, Department of Environmental Engineering, Karabuk, TURKEY*

solution proposals are expected to direct new research areas in the literature [3,4].

On the other side, reactive dyes, which are the colorants of textile products designed to be covalently bonded with cellulosic fibres, are usually used in the textile industry because they offer a wide selection of colour tones, ease of application and brightness [5]. These dyes are of synthetic origin and their complex aromatic form makes them difficult to decompose. Most importantly, textile industries not only generate substantial quantities of wastewater, but this wastewater is also highly concentrated with these dyes [6,7]. It is only when these wastewaters are treated using clean techniques that the damage they cause to the environment could be minimised [8,9]. Hence, it is essential to develop cost-effective and environmentally friendly techniques for the adsorption of toxic dyes.

Today, ecological methods such as green synthesis, in which less toxic reaction by-products are produced and the processes, in which a reduced amount of chemical use is required, have been increasingly implemented in the field of chemistry. For instance, graphene oxide was green-synthesised to treat Methylene Blue (MB) from aquatic solution and it was found that the material presented a great capacity for wastewater treatment [10]. For the adsorption of MB and acid blue, the technique based on the green synthesis of graphene from recycled bottles was applied and it was seen that graphene reveals an outstanding adsorption capacity for several dyes [11]. The MB adsorption capacity of biosynthesised silver nanoparticles was also examined in detail and it was determined that the stability of the material was retained within 60 days [12]. Furthermore, the temperature effect on morphology and transformation of manganese oxide nanoparticles was examined through green synthesis in another study [9].

In this study, aluminium hydroxide sludge, which is a by-product generated from the electroplating and electrochemical industry, was used along with a lavender extract. Lavender (*Lavandula Anguistifolia*) is a plant that grows in temperate climates and is known for its very nice smell and bitter taste. It is also grown in the Mediterranean Region and many places in Turkey [13,14]. Lavender is used for various purposes in the cosmetic, food and medicinal industries due to its rich content [13]. It is stated that lavender has 50.6 mg GA/g phenolic and 27.6 mg R/g flavonoid content [15]. Nanostructures attracted the attention of researchers to better understand the ability to absorb and capturing of chemicals especially water engineering [16]. Nanoparticles such as silver and gold were synthesised by the green synthesising methodology using lavender extract, and antioxidant activity was studied with these nanoparticles [13-17]. For example, gold nanoparticles were synthesised using lavender leaf extract, and their antioxidant capacity was extensively examined [13]. Sea lavender was employed for the green synthesis of zinc oxide nanoparticles to evaluate their microbial and oxidant removal potentials [18]. However, no study has been found so far on the synthesis of nanoparticle-coated adsorbent prepared by green synthesis method using lavender extract, as well as their applicability in dye adsorption. Hence, this study holds originality in this regard.In this study, we propose an environmentally friendly approach for the green synthesis of aluminium hydroxide sludge (AHS) which is produced in large quantities by the galvanising industry. Cu-AHS (Cu-doped AHS) were synthesised using lavender extract under appropriate conditions. The synthesised Cu-doped AHS was then investigated to assess its ability to remove the reactive azo dye RR239 (Reactive Red 239), which was selected as a representative dye in this study. Simultaneously, the kinetic analyses along with the characterisation of Cu-doped AHS before and after dye adsorption provided a deep understanding of its fundamental mechanisms. To the best of our knowledge, based on published literature, this is the first time that Cu-doped AHS was synthesised by using lavender for the removal of textile dye-RR239.

EXPERIMENTAL SECTION

Chemicals

Remazol Red 3BS 133% (Reactive Red 239, RR239), which was purchased from DyStar, is a mono-azo dye with a molecular weight of 1136.32 g/mol. NaOH (CAS: 1310-73-2) and H_2SO_4 (CAS: 7664-93-9) were used for pH adjustment and $CuSO_4.5H_2O$ (CAS: 7758-99-8) obtained from Merck, was utilized for the synthesis of the adsorbent.

Preparation of Cu-doped AHS by Green Synthesis Method

AHS was formed precipitating metal ions from aluminium galvanizing industrial wastewater through alkali precipitation. It was subsequently purified using distilled water, dried, and sieved. AHS with a sieve range of 250-500 µm was used in the study. 40 g of the room-

temperature dried lavender was placed in 1 L of distilled water and stirred at 70 °C for 4 hours. After this blend was kept at room temperature for 18 hours, the lavenders were separated from it with a coarse filter and then the lavender extract was obtained by passing it through 0.45 µm filter paper. 0.5 N solution was prepared by dissolving 78.1 g of $CuSO_4.5H_2O$ in 400 mL distilled water. The lavender extract was heated to 70 °C and 400 mL of 0.5 N Cu solution and 80 g of AHS were added into the extract at the same time. The mixture was stirred at 70 °C for 4 hours and incubated for 18 hours at room temperature in a dark environment. Cu-doped Aluminium Hydroxide Sludge (Cu-AHS) was separated from the extract, and its clumping was eliminated by gently grinding it using a dried mortar at 105 °C.

Adsorption experiments

Adsorption studies were performed by adding Cu-AHS into a 100 mL sample (50 mg/L RR239). The pH value was adjusted by also adding H_2SO_4 and NaOH and it was measured with the help of a pH meter (WTW pH 315i). Adsorption was carried out by 60 minutes of agitation at 150 rpm and samples were taken at 10-minute intervals to determine the RR239 dye removal. After the samples were centrifuged at 4000 rpm for 5 minutes, measurements were recorded by using a spectrophotometer at a wavelength of 542 nm.

In adsorption experiments, the effect of pH on the removal of RR239 dye using Cu-AHS adsorbent was initially investigated. For this purpose, adsorption studies were conducted with 0.1 g of Cu-AHS at a concentration of 50 mg/L RR239 dye, using an agitation speed of 150 rpm, and at five different pH values (3, 5, 7, 9, and 11). Then, R239 dye removal was investigated when pH was 7 and agitation speed was 150 rpm to achieve the highest RR239 uptake by using 8 different Cu-AHS dosages of 0.04, 0.05, 0.06, 0.08, 0.100, 0.135, 0.150 and 0.200 g. To determine the effect of agitation speed on RR239 dye removal, adsorption was performed at 50, 100, 150 and 200 rpm agitation speed with 0.15 g of Cu-AHS at pH 7. In order to determine the effect of RR239 dye concentration, adsorption was performed at 25, 50, 75, 100, 125, 150 and 175 mg/L RR239 dye concentrations at pH 7 with 0.15 g Cu-AHS dosage. In adsorption studies performed on parameters affecting adsorption (pH, Cu-AHS dosage, agitation speed, RR239 concentration), pseudo first and second order kinetics were calculated according to RR239 dye concentration changes obtained with samples taken at 10-minute intervals by employing equations below (Eq. (1) to (3)) [19, 20].

Adsorption Capacity: $$q_{e(adsorption)} = \frac{(C_0 - C_e) * V}{m} \quad (1)$$

Pseudo 1st order kinetic: $$ln(q_e - q_t) = lnq_e - k_1 t \quad (2)$$

Pseudo 2nd order kinetic: $$\frac{t}{q_t} = \frac{1}{k_2 q_e^2} + \frac{1}{q_e} t \quad (3)$$

In Eq. (1), adsorption capacity (q_e) is calculated by using C_0 (mg/L) and C_e (mg/L) which are the initial RR239 concentration, and the equilibrium RR239 concentration respectively. m (g) refers to the amount of adsorbent, and V (L) represents the volume of the dye solution. In Eq. (2) and (3), q_e is the adsorptive removal capacity at equilibrium and q_t (mg/g) is the adsorptive removal capacity at time t (minutes), $k1$ (1/min) and k_2 (g/mg.min) are the rate constants for the first and second order kinetic models.

Adsorption isotherms were conducted at pH 7 by using 0.150 g of AHS or Cu-AHS at initial RR239 concentrations of 25, 50, 75, 100, 125, 150 and 175 mg/L. The adsorption process involved shaking the mixture for 60 minutes at 150 rpm. Samples were taken at 10-minute intervals, followed by centrifugation at 4000 rpm for 5 minutes. The supernatant was then analysed using a spectrophotometer to determine the measurements at a wavelength of 542 nm. In this study, Langmuir and Freundlich Isotherms were calculated with RR239 dye uptake results obtained after 60 minutes of adsorption.

To investigate the effect of temperature on adsorption isotherms, adsorption studies were conducted at temperatures of 20, 30, 35, 40, and 45 °C. The experiments were performed using 0.15 g of Cu-AHS at pH 7 with initial RR239 concentrations of 25, 50, 75, 100, 125, 150, and 175 mg/L. After 60 minutes of adsorption, samples were taken, and the RR239 concentrations in these samples were used to calculate the Langmuir and Freundlich isotherms.

Adsorption thermodynamics were determined based on the RR239 concentrations obtained after 60 minutes of adsorption at temperatures of 20, 30, 35, 40, and 45 °C. The experiments were conducted using a dosage of 0.15 g of Cu-AHS and an initial RR239 dye concentration of 100 mg/L, with pH set at 7.

Analyses

The RR239 dye concentration was specified with the help of a UV–Vis spectrophotometer (Schimadzu

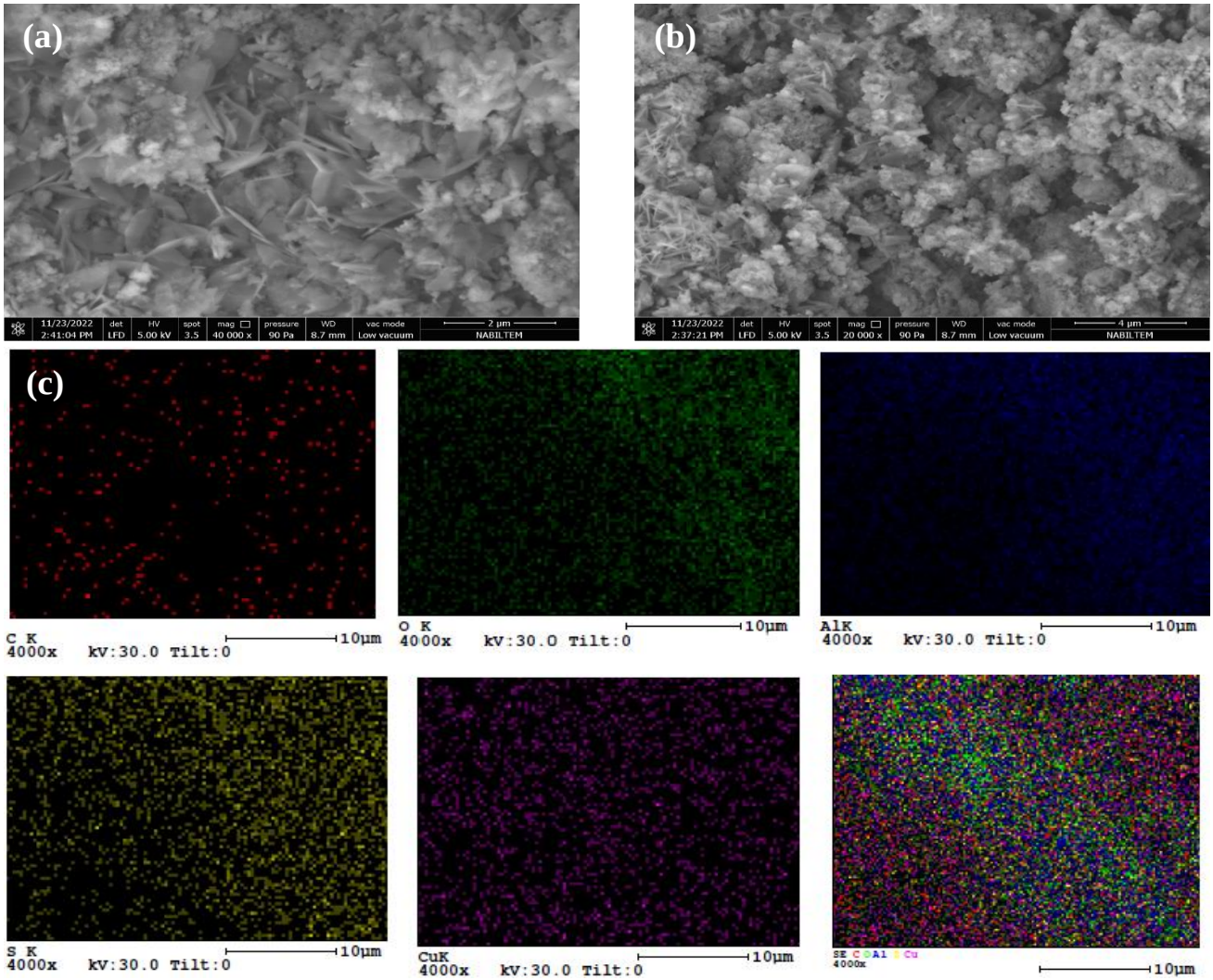

Fig. 1: Characterisation of Cu-AHS a) SEM image of Cu-AHS (2µm), b) SEM image of Cu-AHS (4µm), and c) mapping of Cu-AHS

UV-2401 PC) at a wavelength of 542 nm. SEM, EDAX and mapping were carried out with FEI brand Quanta FEG 250 model device. SEM images were taken at 5 kV, 3.5 spot and 90 Pa pressure with 20000X and 40000X magnifications. A wavelength range of 400 to 4000 (1/cm) was used in the FT-IR (Bruker, Vertex 70 ATR) analysis. Pore volume and specific surface area were calculated in BET analysis which was performed with Micromeritics-Tristar II by N_2 adsorption at 77 K.

RESULTS AND DISCUSSION

Cu-doped AHS Characterisation

The SEM image of Cu-AHS is given in Fig. 1. When the structure of AHS is examined, it was detected that it has crystalline properties in a knife-like structure. This observation aligns with findings reported in the literature [21]. It is seen that the Cu nanoparticle coated with the green synthesis method is heterogeneously located on the AHS surface.

When SEM mapping is examined, it is seen that the distribution of Al and O is similar and heterogeneous, while Cu is distributed homogeneously. In the EDAX analysis of Cu-AHS, the structure of AHS was found to have 9.88±0.56% C (carbon), 63.39±0.63% O (oxygen), 21.94±0.10% Al (aluminium), 4.04±0.14% S (sulphur), whereas Cu-AHS was determined to have 0.75±0.01 of the Cu content by weight.

FT-IR spectrum of Cu-AHS is given in Fig. 2. The highest peaks occur at 1629, 1094, 979, 595, 535 and 478 (1/cm). Sharp large peaks appearing at 478, 535 and 1094 (1/cm) are due to Al-O or Al-O-Al bonds [6,22]. Similarly, in the literature, it was stated that the peaks

Table 1: The results of Cu-AHS's BET analysis

Adsorban	S_{BET} (m^2/g)	S_{micro} (m^2/g)	S_{meso} (m^2/g)	V_{micro} (cm^3/g)	V_{meso} (cm^3/g)	D_p nm
Cu-AHS	38.8948	3.1035	35.7913	0.00137	0.190117	19.69284

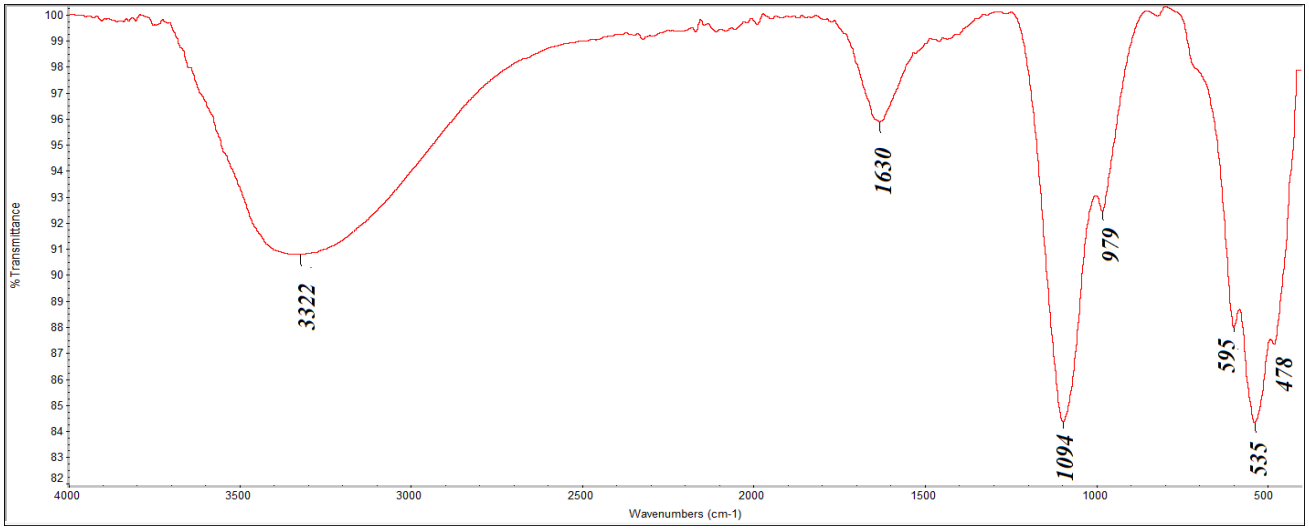

Fig. 2: FT-IR spectrum of Cu-AHS

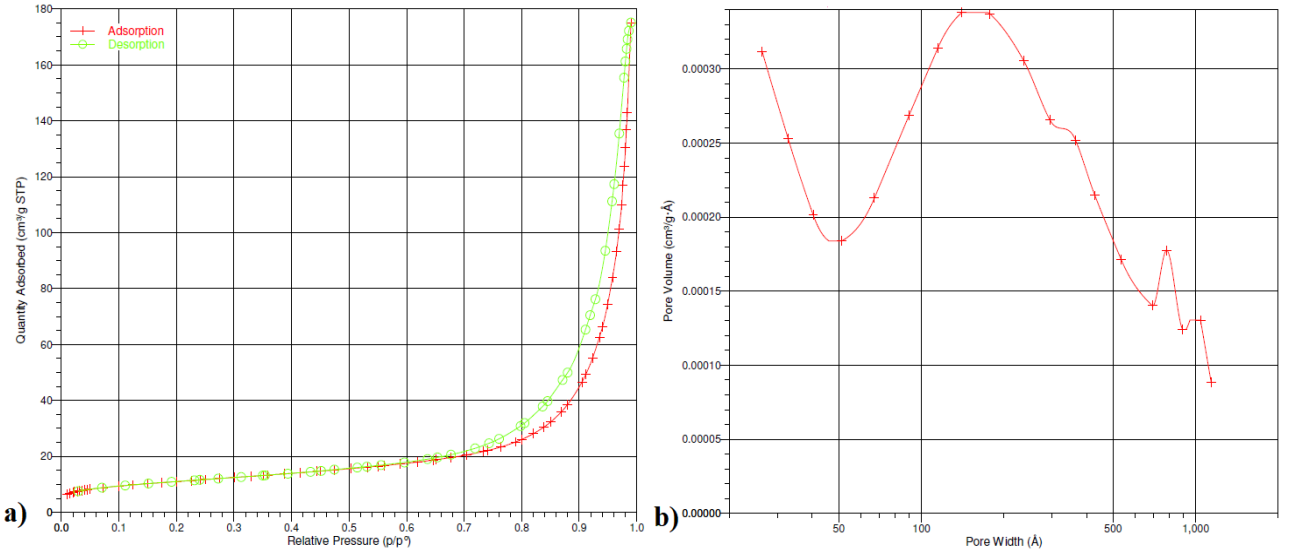

Fig. 3: a) N_2 adsorption-desorption isotherm plot of Cu-AHS b) Pore volume distribution of Cu-AHS

appearing at 510 and 1082 (1/cm) were caused by Al-O bonds of $Al(OH)_3$ [23]. It is estimated that there are vibrations of Cu-O bonds originating from CuO nanoparticles at 478 and 535 (1/cm) [24]. O-H bonds in Cu-AHS are shown at 3322 (1/cm).

BET analysis of Cu-AHS

The results of Cu-AHS's BET analysis are given in Table 1. The specific surface area of Cu-AHS was determined as 38.8948 m^2/g. While Cu-AHS has micro and mesoporous formations, it is seen that it mostly consists of mesoporous structures.

According to the N_2 adsorption-desorption graph, while a small amount of N_2 is adsorbed at low relative pressure ($p/p0 < 0.1$), strong N_2 adsorption is observed at high relative pressure values ($p/p0 > 0.9$) (Fig. 3a). According to the pore volume distribution, it is seen that the majority of Cu-AHS has a pore size of 5-50 nm (Fig. 3b).

Table 2: Kinetic parameters of RR239 dye adsorption with Cu-AHS at different pH values (RR239 concentration: 50 mg/L, Cu-AHS dosage: 1.0 g/L)

pH	q_e (mg/g) (experiment)	Pseudo 1st order			Pseudo 2nd order		
		k_1 (1/min)	q_e (mg/g)	R^2	k_2 (g/mg.min)	q_e (mg/g)	R^2
3	35.97	0.0611	28.66	0.9684	0.003	40.65	0.9978
5	36.49	0.0734	9.40	0.8629	0.034	36.76	0.9996
7	43.74	0.0747	7.55	0.5705	0.063	43.86	0.9999
9	40.91	0.0695	18.96	0.8629	0.011	42.02	0.9994
11	10.03	0.05	6.53	0.8341	0.014	10.79	0.9835

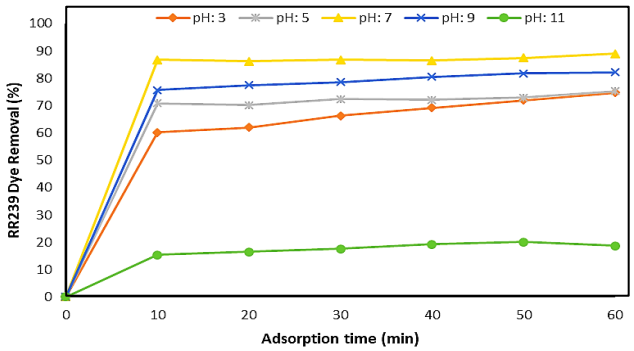

Fig. 4: The effect of pH on RR239 uptake with Cu-AHS (RR239 concentration: 50 mg/L, Cu-AHS dosage: 1.0 g/L)

Effect of pH on dye adsorption and kinetics

pH is a crucial parameter in adsorption studies. Dye adsorption changes depending on both the pH_{pzc} (point of zero charge) of the adsorbent and the charges of dyes [25, 26]. The electrostatic attraction force between the dye and the adsorbent surface plays a significant role in dye adsorption, making the charge of the dye an important factor [27]. In addition, in anionic dyes such as RR239, the position of SO_3 and NH_2 groups affects the dye adsorption due to the amount of positively charged sulfonic groups with affinity and affects the electrostatic power [25, 28].

In studies conducted at different pH values, the lowest RR239 uptake was 18.7% at pH 11, while it was reported that RR239 uptake increased as the pH value decreased to 7 (Fig. 4). It is stated that RR239 dye uptake is quite low at pH 11 compared to other pH values is due to ionic repulsion as a consequence of the existence of OH ions between negatively charged Cu-AHS and aprotic dye molecules [25]. Extremely low removal of the anionic reactive dye RR239 under strongly basic (pH 10-11) conditions has also been observed in the literature [26].

At pH 9, the uptake of RR239 increased to 82.2%, while at pH 7, the uptake reached 89.0%. A decrease in RR239 uptake was observed at acidic pH values (pH<7), with a decrease of up to 67.7% at pH 3. Cu-AHS exhibited the maximum uptake of RR239 dye at pH 7, whereas the optimum pH for RR239 dye uptake with modified zeolite was also found to be pH 7 [25].

Pseudo 1st and 2nd order kinetic parameters calculated at different pH values are depicted in Table 2. It is seen that the RR239 dye adsorption with Cu-AHS takes place rapidly in the first 10 minutes of adsorption time and after 10 minutes the RR239 adsorption is quite slow. Cu-AHS for RR239 dye uptake consists of two stages: the first is the initial phase, in which the adsorption of RR239 dye molecules is fast, and the second is the slow adsorption of RR239 dye molecules [25]. RR239 dye adsorption with Cu-AHS is more suited to pseudo 2nd order kinetics, and the highest q_e and k_2 were obtained with pseudo 2nd order kinetics at pH 7 as 43.86 mg/g and 0.063 g/(mg.min), respectively. While the pseudo 2nd order kinetic represents the linear relationship of the adsorption rate with adsorbent concentration and the adsorbate, the dosage of adsorbent becomes an essential factor [7].

Effect of Cu-AHS dosage on the dye adsorption and kinetics

The time-dependent RR239 dye uptake at different Cu-AHS dosages at pH 7 is given in Fig. 5. As Cu-AHS dosage increased up to 1.5 g/L, RR239 uptake also improved, but no significant change was observed in RR239 dye removal with increasing Cu-AHS dosage to 2.0 g/L. The RR239 dye uptake was 41.1% at a Cu-AHS dosage of 0.4 g/L. As the Cu-AHS dosage increased to 0.6, 0.8, and 1.0 g/L, the RR239 dye uptake increased to 74.5%, 87.4%, and 89.0%, respectively. Achieving a dosage of 1.50 g/L Cu-AHS resulted in a RR239 dye uptake of 95.7%. The progression in the adsorption of MB (Methylene Blue) with the increase of Cu-AHS dosage from 0.4 to 1.5 g/L causes a growth in the effective surface zone of Cu-AHS [29].

Table 3: Kinetic parameters of RR239 dye adsorption with Cu-AHS at different Cu-AHS dosage (RR239 concentration: 50 mg/L, pH: 7)

Cu-AHS dosage (g/L)	q_e (mg/g) (experiment)	Pseudo 1st order			Pseudo 2nd order		
		k_1 (1/min)	q_e (mg/g)	R^2	k_2 (g/mg.min)	q_e (mg/g)	R^2
0.4	51.32	0.0695	10.91	0.5486	0.026	52.36	0.9993
0.5	46.14	0.1074	23.86	0.9323	0.017	47.17	0.9999
0.6	62.07	0.0761	53.93	0.9471	0.002	69.93	0.9908
0.8	46.55	0.0720	38.29	0.9476	0.003	52.36	0.9908
1.0	44.49	0.0579	8.66	0.5048	0.036	44.44	0.9995
1.35	34.09	0.0569	20.05	0.8839	0.006	35.97	0.9979
1.50	31.89	0.1066	5.04	0.6693	0.704	31.85	1.0000
2.00	24.06	0.0838	1.75	0.4497	0.494	24.04	1.0000

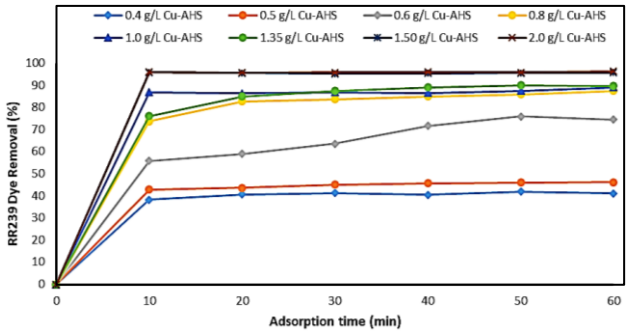

Fig. 5: The effect of Cu-AHS dosage on RR239 uptake (RR239 concentration: 50 mg/L, pH: 7)

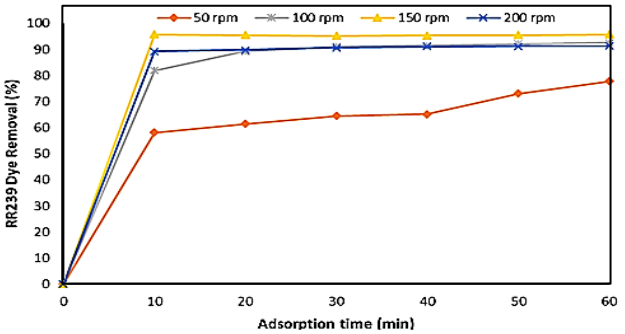

Fig. 6: The effect of agitation speed on RR239 removal with Cu-AHS (RR239 concentration: 50 mg/L, Cu-AHS: 1.5 g/L, pH: 7)

The kinetic parameters acquired in the study performed at changing Cu-AHS dosages are given in Table 3. It is seen that RR239 dye adsorption is more suited to pseudo 2nd order kinetics at all Cu-AHS dosages. Pseudo 2nd order kinetics show that the rate-limiting step is chemical adsorption between the surface of the Cu-AHS and the RR239 dye molecules [30]. At the dosages of 1.5 g/L Cu-AHS with the highest RR239 dye uptake, q_e and k_2 were calculated as 31.85 mg/g and 0.704 g/mg.min, respectively.

Effect of agitation speed on dye adsorption and kinetics

To determine the effect of agitation speed on RR239 adsorption, RR239 dye removals obtained in studies performed with Cu-AHS at different agitation speeds are given in Fig. 6. As seen in the figure, while 77.8% RR239 dye removal was obtained after 60 minutes of adsorption at 50 rpm agitation speed, RR239 dye removal increased to 92.6% at 100 rpm agitation speed. By agitation, the diffusion and mass transfer coefficient increase and the boundary resistance on the Cu-AHS surface decreases, so the RR239 dye removal improves [31].

While the highest RR239 dye removal rate was obtained as 95.7% at 150 rpm agitation speed, RR239 dye removal decreased to 91.2% when this speed increased to 200 rpm. High agitation speed causes the collision of RR239 dye and Cu-AHS with increasing kinetic energy, and as a result, RR239 dye molecules on the Cu-AHS surface are mixed into the solution by desorption [32]. The kinetic parameters obtained at different agitation speeds are given in Table 4. Parallel to the removal efficiency, q_{max} and k_2 increase at 100 and 150 rpm agitation speed and decrease at 200 rpm.

Effect of initial dye concentrations on the dye adsorption and kinetics

The concentration of the dye plays a significant role in dye adsorption as it facilitates mass transfer between the liquid and solid phases. The dye concentration acts as a driving force to overcome resistance and thus affects dye adsorption [27]. The time-dependent variation of Cu-AHS for RR239 dye uptake at different initial RR239 dye concentrations is given in Fig. 7. While around 95% RR239 uptake was achieved at 25 and 50 mg/L RR239

Table 4: Kinetic parameters of RR239 dye adsorption with Cu-AHS at different agitation speed (RR239 concentration: 50 mg/L, Cu-AHS: 1.5 g/L, pH: 7)

Agitation speed (rpm)	q_e (mg/g) (experiment)	Pseudo 1st order			Pseudo 2nd order		
		k_1 (1/min)	q_e (mg/g)	R^2	k_2 (g/mg.min)	q_e (mg/g)	R^2
50	25.93	0.0445	16.64	0.8382	0.005	27.62	0.9808
100	30.85	0.1002	14.64	0.9282	0.023	31.55	1.0000
150	31.89	0.1066	5.04	0.6693	0.704	31.85	1.0000
200	30.41	0.1212	8.15	0.8703	0.092	30.58	1.0000

Table 5: Kinetic parameters of RR239 dye adsorption with Cu-AHS at different initial RR239 dye concentration (Cu-AHS: 1.5 g/L, pH: 7)

Initial RR239 (mg/L)	q_e (mg/g) (experiment)	Pseudo 1st order			Pseudo 2nd order		
		k_1 (1/min)	q_e (mg/g)	R^2	k_2 (g/mg.min)	q_e (mg/g)	R^2
25	16.55	0.0165	0.53	0.0164	0.866	16.58	1.0000
50	32.87	0.1029	1.22	0.4424	1.320	32.89	1.0000
75	46.60	0.736	21.06	0.8653	0.011	47.85	0.9997
100	48.25	0.0990	18.08	0.8822	0.023	49.02	0.9999
125	39.27	0.0934	8.00	0.7216	0.015	39.53	1.0000
150	45.56	0.0741	13.70	0.7523	0.023	46.08	0.9998
175	48.35	0.1140	18.51	0.8922	0.029	48.78	0.9999

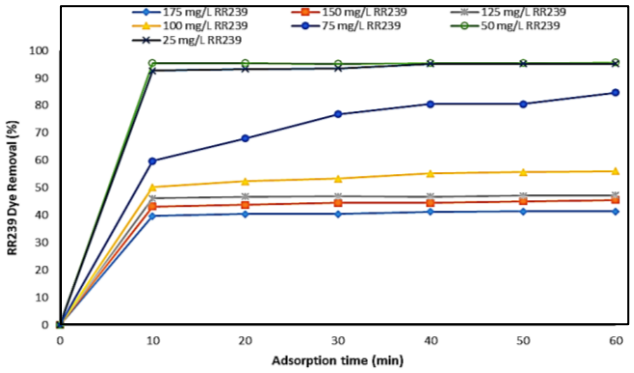

Fig. 7: The effect of initial RR239 concentration on RR239 uptake with Cu-AHS (Cu-AHS: 1.5 g/L, pH: 7)

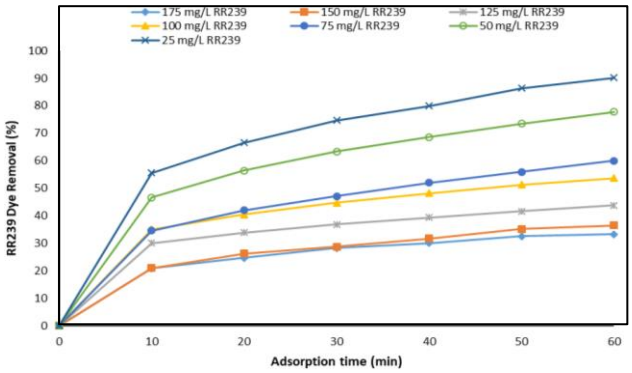

Fig. 8: The effect of initial RR239 concentration on RR239 uptake with AHS (AHS: 1.5 g/L, pH: 7)

dye concentration, a gradual decrease in RR239 uptake was experienced after 75 mg/L initial RR239 concentration. While 95.7% RR239 dye uptake was seen at 50 mg/L RR239 dye concentration, RR239 dye uptake decreased to 41.4% at 175 mg/L RR239 dye concentration. At low initial RR239 dye concentrations, the dyes in the solution interrelate with the binding sites, resulting in improved adsorption, while at high initial RR239 dye concentrations, the RR239 dye uptake efficiency decreases due to the saturation of active sites [31].

When the kinetic analysis is examined at different initial concentrations of RR239, it was experienced that the pseudo 2nd order kinetics suited more for RR239 dye uptake (Table 5). While the highest k_2 value was obtained as 1.32 g/mg.min at 50 mg/L RR239 dye concentration, the k_2 value sharply decreased at 75 mg/L RR239 dye concentration.

To compare the RR239 dye uptake of Cu-AHS and AHS adsorbents, time-dependent dye removal studies were conducted at pH 7 using 1.5 g/L AHS with RR239 dye concentrations ranging from 25 to 175 mg/L. Unlike the Cu-AHS adsorbent, it was observed that the RR239 dye uptake increased over time in the studies conducted with the AHS adsorbent (Fig. 8). However, in the first 10 min of adsorption with Cu-AHS, there was a significant reduction in RR239 dye uptake, and no substantial change was observed in the subsequent periods.

Table 6: Kinetic parameters of RR239 dye adsorption with AHS at different initial RR239 dye concentration (AHS: 1.5 g/L, pH: 7)

Initial RR239 (mg/L)	q_e (mg/g) (experiment)	Pseudo 1st order			Pseudo 2nd order		
		k_1 (1/min)	q_e (mg/g)	R^2	k_2 (g/mg.min)	q_e (mg/g)	R^2
25	16.43	0.0858	5.45	0.8265	0.671	16.61	0.9999
50	30.94	0.0714	14.07	0.8679	0.016	31.75	0.9995
75	41.12	0.0656	20.64	0.8778	0.009	42.55	0.9990
100	47.26	0.0668	27.02	0.9124	0.006	49.50	0.9988
125	36.53	0.0534	27.33	0.9560	0.003	40.49	0.9942
150	36.55	0.0578	34.60	0.9457	0.023	43.67	0.9900
175	38.87	0.0675	37.30	0.9463	0.002	45.05	0.9958

Table 7: Langmuir and Freundlich Isotherm constants of RR239 with AHS and Cu-AHS (AHS or Cu-AHS: 1.5 g/L, pH: 7, time: 60 min)

Parameter	AHS	Cu-AHS
Langmuir Isotherm		
q_{max} (mg/g)	37.88	47.39
K_L (L/mg)	1.7	3.7
R_L	0.006-0.023	0.006-0.011
R^2	0.9978	0.9985
Freundlich Isotherm		
1/n	0.1291	0.1395
K_F	22.52	28.30
R^2	0.7452	0.7379
Temkin Isotherm		
B	3.90	4.35
A_T (L/g)	626	1280
R^2	0.6439	0.7930

In the adsorption studies of RR239 with Cu-AHS, a dye uptake of 95% was achieved for dye concentrations up to 50 mg/L. In the studies conducted with AHS, it was observed that the dye uptake decreased from 90.2% to 77.8% by increasing the RR239 dye concentration from 25 mg/L to 50 mg/L. At 75 mg/L RR239 dye concentration, 84.7% and 60.0% RR239 dye uptake rates were obtained with Cu-AHS and AHS, respectively. With the 75 mg/L RR239 dye concentration, a great reduction in RR239 dye removal was observed with Cu-AHS adsorbent. At all RR239 dye concentrations, the dye removal rates obtained with Cu-AHS were higher than those acquired with AHS.

The kinetic parameters obtained in the AHS and RR239 dye adsorption studies are given in Table 6. Compared to Cu-AHS, it is seen that the k_2 values obtained with AHS are lower, and the highest k_2 was obtained as 0.671 g/mg.min at 25 mg/L RR239 dye concentration. With Cu-AHS, the k_2 value increases up to 50 mg/L RR239 dye concentration, and the k_2 value was calculated as 1.320 g/(mg.min) at 75 mg/L RR239 concentration.

Adsorption isotherms

Langmuir, Freundlich and Temkin isotherm models were created with the RR239 dye uptake results obtained with Cu-AHS and AHS at different concentrations of RR239. These isotherm models were calculated according to the formulations given in our previously published AHS study [5,6,33]. The parameters obtained for RR239 dye adsorption with AHS and Cu-AHS are presented in Table 7. As shown in the table, the dye adsorption of AHS and Cu-AHS for RR239 uptake is more suitable for the Langmuir isotherm since the R^2 value is closer to 1.

The adsorption of AHS and Cu-AHS for RR239 uptake takes place as a single layer on the homogeneous adsorbent surface [6]. In the range of 25-175 mg/L RR239 initial dye concentration, the K_L value calculated for Cu-AHS and AHS adsorbents was between 0 and 1, indicating that RR239 dye adsorption with these adsorbents is favourable [6]. Similarly, the 1/n value between 0 and 1 in the Freundlich isotherm indicates that the RR239 dye adsorption with AHS and Cu-AHS adsorbents is also favourable [8]. According to Langmuir isotherm, q_{max} values for AHS and Cu-AHS with RR239 were obtained as 37.88 and 47.39 mg/g, respectively. It was noted that the q_{max} value improved 1.25 times in RR239 dye adsorption with Cu-AHS adsorbent made by the green synthesis method with lavender extract. Previously, q_{max} was calculated as 55.2 mg/g with AHS in the 100-500 µm size range [6]. However, since AHS in the 250-500 µm size range was used in this study, it is thought that an increase in AHS particle size causes a decrease in RR239 dye adsorption capacity. In addition, in the SEM-EDAX analysis

Table 8: Isotherm parameters obtained in the uptake of RR239 dye with different adsorbents

Adsorban	Conditions	Langmuir Isotherm				Freundlich Isotherm			Ref.
		q_{max} (mg/g)	K_L (L/g)	R_L	R^2	K_F	n	R^2	
AHS	C: 25-175 mg/L, pH: 7, dosage: 1.5 g/L	37.88	1.7	0.006-0.023	0.9978	22.52	7.75	0.7452	this study
Cu-AHS	C: 25-175 mg/L, pH: 7, dosage: 1.5 g/L	47.39	3.7	0.006-0.011	0.9985	28.30	7.17	0.7379	this study
AHS	C: 100-1000 mg/L, pH: 5, dosage: 8 g/L	55.2	0.134	0.007-0.130	0.9869	2.30	0.018	0.9049	[6]
HDMA-zeolite	C: 25-500 mg/L, pH: 7, dosage: 0.05 g	33.0	$3.22.10^3$	0.383	0.9886	$17.55.10^2$	0.8188	0.9975	[25]
HTAB-zeolite	-	111.1	1.088	0.0098	0.98				[34]
Fe_3O_4@CS-BAL	C: 40-160 mg/L, pH: 7, dosage: 20 mg	200	2.5	0.0039	0.9969	7.93	6.32	0.8526	[26]
AAm-AAc hydrogel	C: 30-300 mg/L, dosage: 0.2 g	44.19	$6.93.10^{-3}$	-	0.9901	-	-	-	[35]
Sepiolite	-	108.8	2.31	0.021	0.97	-	-	-	[36]
Zeolite	-	111.1	0.919	0.009	0.98	-	-	-	
Corra sawdust	C: 50-300 mg/L, pH: 1.6, dosage: 83.3 g/L	15.1	0.0183	-	0.99	0.305	1.14	0.99	[37]

HDMA-zeolite: hexamethylenediamine modified zeolite, HTAB-zeolite: hexadecyltrimethylammonium bromide modified zeolite, AAm-AAc hydrogel: Acrylamide and acrylic acid hydrogel

Table 9: Langmuir and Freundlich Isotherm constants of RR239 with Cu-AHS (Cu-AHS: 1.5 g/L, pH: 7, time: 60 min)

Parameter	20 °C	30 °C	35 °C	40 °C	45 °C
Langmuir Isotherm					
q_{max} (mg/g)	47.39	64.94	64.52	74.07	73.53
K_L (L/mg)	3.7	0.1	0..2	0.1	0.1
R_L	0.006-0.011	0.006-0.212	0.006-0.190	0.006-0.270	0.006-0.239
R^2	0.9985	0.9922	0.9939	0.9956	0.9964
Freundlich Isotherm					
1/n	0.1395	0.2767	0.2586	0.2972	0.2716
K_F	28.30	19.34	21.14	19.36	21.86
R^2	0.7379	0.8406	0.8404	0.9221	0.9776

Table 10: Thermodynamic parameters of RR239 dye adsorption with Cu-AHS (RR239: 100 mg/L, pH: 7, Cu-AHS: 1.5 g/L, time: 60 min)

Cu-AHS	ΔH° (kJ/mol)	ΔS° (kJ/mol)	ΔG° (kJ/mol)				
			20 °C	30 °C	35 °C	40 °C	45 °C
RR239	8.4309	33.7236	-1.36	-1.94	-2.00	-2.11	-2.22

performed in the above-mentioned study, it was determined that the aluminium content was 25.55% and it contained trace amounts of silicon and iron. In this study, the aluminium content in AHS was noted as 21.94%, and the silicon and iron content was not found.

The comparison of the isotherm parameters obtained in RR239 dye adsorption studies with AHS and Cu-AHS adsorbents, as well as various adsorbents reported in the literature, is presented in Table 8. When Table 8 is taken into consideration, it was determined that RR239 dye adsorption with different adsorbents was generally more suitable to the Langmuir isotherm. In addition, it is noted in Table 8 that the q_{max} value obtained with Cu-AHS is higher than HDMA-zeolite, AAm-AAc hydrogel and Corra sawdust adsorbents.

Effect of temperature on adsorption isotherms

The isotherm parameters calculated at different temperatures to evaluate the effect of temperature on adsorption isotherms are given in Table 9. The results indicate that the Langmuir Isotherm model is more appropriate as the R^2 value is closer to 1 across all temperature values.

When examining the q_{max} values calculated in the Langmuir isotherm model, it is observed that these values also increase with rising temperature. While the q_{max} value increases from 47.39 mg/g to 64.52 mg/g with an increase in temperature from 20°C to 30°C, q_{max} improves to 74.07 mg/g with an increase in temperature to 40°C. However, at 45°C, there is a slight decrease in the q_{max} value.

Adsorption thermodynamics

Adsorption thermodynamics were calculated based on the RR239 dye removals achieved at various temperatures using 0.15 g of Cu-AHS at a concentration of 100 mg/L RR239 dye, pH 7. The calculated thermodynamic parameters are presented in Table 10. To determine these parameters, the Van't Hoff equation graph of 1/T versus ln K_d was drawn with the help of formulas in the literature, and ΔH° from the equation slope and ΔS° from the

intersection were determined [38]. The positive ΔH° (enthalpy change) indicates that the adsorption of Cu-AHS and RR239 is endothermic. Positive ΔS° (entropy change) shows the increase in the randomness and disorder of the adsorbent surface after adsorption, while negative ΔG° (free energy change) indicates the spontaneity and feasibility of the adsorption process [38].

CONCLUSIONS

Green synthesis of Cu-AHS with lavender for the treatment of RR239 has been applied in this study and the effect of pH, Cu-AHS dosage and initial dye concentration on the adsorption process was tested experimentally. It was seen that the lowest RR239 uptake was 18.7% at pH 11, while it increased as the pH value decreased to 7. It was specified that at a dosage of 1.50 g/L Cu-AHS, 95.7% RR239 dye uptake was achieved. It was also determined that RR239 dye adsorption with Cu-AHS was more suitable for pseudo second order kinetics.

SEM and FT-IR analyses showed that the structure of AHS has crystalline properties in a knife-like structure and the Cu nanoparticle coated with the green synthesis method is heterogeneously located on the AHS surface. It was seen that AHS is in the form of aluminium hydroxide and the structure of AHS has 9.88±0.56% C, 63.39±0.63% O, 21.94±0.10% Al, 4.04±0.14% S content, whereas Cu-AHS has 0.75±0.01 Cu content by weight.

The results of BET analysis show that Cu-AHS mostly consists of mesoporous structures. For the comparison of the RR239 dye uptake capacities of two materials, Cu-AHS adsorbent and AHS adsorbent, time-dependent uptake studies were conducted at pH 7 and 1.5 g/L AHS concentration in the range of 25-175 mg/L RR239 dye concentration. It was observed that even though there was a great decrease in RR239 dye uptake with Cu-AHS adsorbent after 75 mg/L dye concentration, higher RR239 dye uptake was reached at all RR239 dye concentrations with Cu-AHS compared to those acquired with AHS. Adsorption isotherms also showed that the dye adsorption of AHS and Cu-AHS with RR239 is more suited to the Langmuir isotherm since the R^2 value is closer to 1.

Considering that AHS is a waste formed by metal precipitation in aluminium galvanising industry, the use of AHS as an adsorbent material is of great importance in terms of the reusability of the waste. Furthermore, the cost of the adsorbent material is a crucial factor influencing the overall cost of the adsorption process. By employing aluminium hydroxide sludge as a low-cost adsorbent, the expenses associated with wastewater treatment through adsorption can be reduced. The adoption of the green synthesis method, which is the state-of-the-art approach in this study, offers an alternative avenue for treating RR239 present in textile wastewater, eliminating potential environmental hazards associated with conventional treatment methods.

Received: Mar. 02, 2023; Accepted: Jun. 26, 2023

REFERENCES

[1] Filho W.L., Saari U., Fedoruk M., lital A., Moora H., Klöga M., Voronova V., An Overview of the Problems Posed by Plastic Products and the Role of Extended Producer Responsibility in Europe, *Journal of Cleaner Production*, **214(20):** 550-558 (2019).

[2] Cai Y.J., Choi T.M., Extended Producer Responsibility: A Systematic Review and Innovative Proposals for Improving Sustainability, *IEEE Transactions on Engineering Management*, **68(1):** 272-288 (2021).

[3] Shooshtarian S., Maqsood T., Wong P.S.P., Khalfan M., Yang R.J., Extended Producer Responsibility in the Australian Construction Industry, *Sustainability*, **13**(2):620 (2021), https://doi.org/10.3390/su13020620

[4] Maitre-Ekern E., Re-Thinking Producer Responsibility for a Sustainable Circular Economy from Extended Producer Responsibility to Pre-Market Producer Responsibility, *Journal of Cleaner Production*, **286(1):** 125454 (2021).

[5] Cifci D.I., Aydin N., Atav R., Gunes Y., Gunes E., Synthesis of $ZnCl_2$ Activated Raising Powder of Cotton Fabrics for Acid and Basic Dye Adsorption: A Way to Reuse Cellulosic Wastes for Sustainable Production, *Journal of Natural Fibers*, **19(16):** 14299-14317 (2022).

[6] Aydın N., Cifci D.I., Gunes E., Gunes Y., Atav R., Decolorization Potential of Reactive Dyes by Using Galvanising Industry's Waste (Aluminum Hydroxide Sludge) Depending on Dye Chromophore, *Journal of the Textile Institute*, **114(9):** 1301-1310 (2022).

[7] Hussain Z., Chang N., Sun J., Xiang S., Ayaz T., Zhang H., Wang H., Modification of Coal Fly Ash and Its Use as Low-Cost Adsorbent for the Removal of Directive, Acid and Reactive Dyes, *Journal of Hazardous Materials*, **422**:126778 (2022).

[8] Aydın N., Çifçi D.I. Comparison of Conventional and Ultrasonic-Assisted Adsorption Processes by Using H_3PO_4 Activated Cypress Tree Cone for Methylene Blue Removal, *J. Wat. Chem. Tech.*, **44(4):** 269–279 (2022).

[9] Patra T., Mohanty A., Singh L., Muduli S., Parhi P.K., Sahoo T.R., Effect of Calcination Temperature on Morphology and Phase Transformation of MnO_2 Nanoparticles: A Step Towards Green Synthesis for Reactive Dye Adsorption, *Chemosphere*, **288(2):** 132472 (2022).

[10] Gan L., Li B., Chen Y., Yu B., Chen Z., Green Synthesis of Reduced Graphene Oxide Using Bagasse and its Application in Dye Removal: A Waste-to-Resource Supply Chain, *Chemosphere*, **219:** 148-154 (2019).

[11] El-Essawy N.A., Ali S.M., Farag H.A., Konsowa A.H., Elnouby M., Hamad H.A., Green Synthesis of Graphene from Recycled PET Bottle Wastes for Use in the Adsorption of Dyes in Aqueous Solution, *Ecotox. Envir. Safe.*, **145:** 57-68 (2017).

[12] Rohaizad A., Shahabuddin S., Shahid M.M., Rashid N.M., Hir A.M., Ramly M.M., Awang K., Siong W.S., Aspanut Z., Green Synthesis of Silver Nanoparticles from Catharanthus Roseus Dried Bark Extract Deposited on Graphene Oxide for Effective Adsorption of Methylene Blue Dye, *J. Envir. Chem. Eng.*, **8(4):** 103955 (2020).

[13] Kumar B., Smita K., Vizuete K.S., Cumbal L ., Aqueous Phase Lavender Leaf Mediated Green Synthesis of Gold Nanoparticles and Evaluation of Its Antioxidant Activity, *Bio. Med.*, **8(3):** (2016).

[14] Kumar B., Smita K., Cumbal L., Biosynthesis of Silver Nanoparticles Using Lavender Leaf and their Applications for Catalytic, Sensing, and Antioxidant Activities, *Nanotechnol Rev*, **5(6):** 521–528 (2016).

[15] Spiridon I., Colceru S, Anghel N., Teaca C.A., Bodirlau R., Armatu A., Antioxidant Capacity and Total Phenolic Contents of Oregano (Origanum Vulgare), Lavender (Lavandula Angustifolia) and Lemon Balm (Melissa Officinalis) from Romania, *Nat. Prod. Res*., **25:** 1657–166 (2011).

[16] Sabet M., Tanreh S., Khosravi A., Astaraki M., Rezvani M., Ganji M.D., Theoretical Assessment of the Solvent Effect on the Functionalization of Au32 and C60 Nanocages with Fluorouracil Drug, *Diam. Rela. Mater.*, **126:** 109142 (2022).

[17] Baláž M., Bedlovičová Z., Daneu N., Siksa P., Sokoli L., Tkáčiková L., Salayová A., Džunda R., Kováčová M., Bureš R., Bujňáková Z.L., Mechanochemistry as an Alternative Method of Green Synthesis of Silver Nanoparticles with Antibacterial Activity: A Comparative Study, *Nanomaterials*, **11:** 1139 (2021).

[18] Naiel B., Fawzy M., Halmy M.W.A., Mahmoud A.E.D., Green Synthesis of Zinc Oxide Nanoparticles using Sea Lavender (Limonium Pruinosum L. Chaz.) Extract: Characterization, Evaluation of Anti-Skin Cancer, Antimicrobial and Antioxidant Potentials, *Sci. Rep.*, **12:** 20370 (2022).

[19] Wang J., Guo X., Adsorption Kinetic Models: Physical Meanings, Applications, and Solving Methods, *J. Hazard. Mater*, **390:** 122156 (2020).

[20] Cifci D.I., Aydın N., Comparison of H_3PO_4 and $ZnCl_2$ Activated Filtered Coffee Waste Carbon-based Adsorbents in Methylene Blue Removal by Using Ultrasonic-Assisted Adsorption, *Arabian Journal for Science and Engineering*, **48:** 8641-8653 (2022).

[21] Anjum M.J., Zhao J., Asl V.Z., Yasin G., Wang W., Wei S., Zhao Z., Khan W.Q., In-Situ Intercalation of 8-Hydroxyquinoline in Mg-Al LDH Coating to Improve the Corrosion Resistance of AZ31, *Corrosion Science*, **157:** 1-10 (2019).

[22] Jeon E.-K., Ryu S., Park S.-W., Wang L., Tsang D.C.W., Baek K., Enhanced Adsorption of Arsenic onto Alum Sludge Modified by Calcination, *Journal of Cleaner Production*, **176:** 54-62 (2018).

[23] González-Gómez M.A., Belderbos S., Yañez-Vilar S., Piñeiro Y., Cleeren F., Bormans G., Deroose C.M., Gsell W., Himmelreich U., Rivas J., Development of Superparamagnetic Nanoparticles Coated with Polyacrylic Acid and Aluminum Hydroxide as an Efficient Contrast Agent for Multimodal Imaging, *Nanomaterials*, **9:** 1626 (2019).

[24] Sathish, Rafi S.M., Shaik H., Madhavi P., Kosuri Y.R., Sattar S.A., Kumar K.N., Critical Investigation on Cu-O Bonding Configuration Variation in Copperoxide Thin Films for Low-Cost Solar Cell Applications, *Mater. Sci. Semic. Proc.*, **96:** 127-131 (2019).

[25] Alver E., Metin A.U., Anionic Dye Removal from Aqueous Solutions Using Modified Zeolite: Adsorption Kinetics and Isotherm Studies, *Chemical Engineering Journal*, **200(202):** 59–67 (2012).

[26] Banaei A., Yaychi M.F., Karimi S., Vojoudi H., Namazi H., Badiei A., Pourbasheer E., 2,2'-(Butane-1,4-Diylbis(Oxy))Dibenzaldehyde Cross-Linked Magnetic Chitosan Nanoparticles as a New Adsorbent for the Removal of Reactive Red 239 from Aqueous Solutions, *Materials Chemistry and Physics*, **212:** 1-11 (2018).

[27] Shukor H., Yaser A.Z., Shoparwe N.F., Makhtar M.M.Z., Mokhtar N., Biosorption Study of Methylene Blue (MB) and Brilliant Red Remazol (BRR) by Coconut Dregs, *International Journal of Chemical Engineering*, **11:** 8153617 (2022).

[28] Netpradit S., Thiravetyan P., Towprayoon S., Application of Waste Metal Hydroxide Sludge for Adsorption of Azo Reactive Dyes, *Water Res*., **37:** 763–772 (2003).

[29] Shojaei S., Nouri A., Baharinikoo L., Farahani M.D., Shojaei S., Removal of the Hazardous Dyes through Adsorption over Nanozeolite-X: Simultaneous Model, Design and Analysis of Experiments, *Polyhedron*, **196:** 114995 (2021).

30] Bapat S., Jaspal D., Malviya A., Efficacy of Parthenium Hysterophorus Waste Biomass Compared with Activated Charcoal for the Removal of CI Reactive Red 239 Textile Dye from Wastewater, *Voloration Technology*, **137(3):** 234-250 (2021).

[31] Islam M.R., Mostafa M.G., Adsorption Kinetics, Isotherms and Thermodynamic Studies of Methyl Blue in Textile Dye Effluent on Natural Clay Adsorbent, *Sustain. Water Resour. Manag*, **8:** 52 (2022).

[32] Kulkarni P, Watwe V., Chavan T., Kulkarni S., Artificial Neural Networking for Remediation of Methylene Blue Dye Using Fuller's Earth Clay, *Current Research in Green and Sustainable Chemistry*, **4:** 100131 (2021).

[33] Güneş E., Kaygusuz T., Adsorption of Reactive Blue 222 onto an Industrial Solid Waste Included Al(III) Hydroxide: pH, Ionic Strength, Isotherms, and Kinetics Studies, *Desalination and Water Treatment*, **53(9):** 2510-2517 (2015).

[34] Armağan B., Özdemir O., Turan M., Çelik M.S., The Removal of Reactive Azo Dyes by Natural and Modified Zeolites, *J. Chem. Technol. Biotechnol.*, **78:** 725-732 (2003).

[35] Corona-Rivera M.A., Ovando-Medina V.M., Bernal-Jacome L.A., Cervantes-González E., Antonio-Carmona I.D., Dávila-Guzmán N.E., Remazol Red Dye Removal Using Poly (Acrylamide-Co-Acrylic Acid) Hydrogels and Water Absorbency Studies, *Colloid. Polym. Sci.*, **295:** 227-236 (2017).

[36] Özdemir Ö., Armagan B., Turan M., Çelik M.S., Comparison of the Adsorption Characteristics of Azo-Reactive Dyes on Mezoporous Minerals, *Dyes and Pigments*, **62:** 49–60 (2004).

[37] Sanchez N., Benedetti T.M., Vazquez M., Córdoba de Torresi S.I., Torresi R.M., Kinetic and Thermodynamic Studies on the Adsorption of Reactive Red 239 by Carra Sawdust Treated with Formaldehyde, *Adsorption Science & Technology*, **30(10):** 881-899 (2012).

[38] Sahu S., Pahi S., Tripathy S., Singh K., Behera A., Sahu U.K., Patel R.K., Adsorption of Methylene Blue on Chemically Modified Lychee Seed Biochar: Dynamic, Equilibrium, and Thermodynamic Study, *Journal of Molecular Liquids*, **315:** 113743 (2020).